Victoriia NAUMENKO, Bogdan KOVALENKO, Volodymyr LUKIN

National Aerospace University "Kharkiv Aviation Institute", Kharkiv, Ukraine

BPG-BASED COMPRESSION ANALYSIS OF POISSON-NOISY MEDICAL IMAGES

*The **subject matter** is lossy compression using the BPG encoder for medical images with varying levels of visual complexity, which are corrupted by Poisson noise. The **goal** of this study is to determine the optimal parameters for image compression and select the most suitable metric for identifying the optimal operational point. The **tasks** addressed include: selecting test images sized 512x512 in grayscale with varying degrees of visual complexity, encompassing visually intricate images rich in edges and textures, moderately complex images with edges and textures adjacent to homogeneous regions, and visually simple images primarily composed of homogeneous regions; establishing image quality evaluation metrics and assessing their performance across different encoder compression parameters; choosing one or multiple metrics that distinctly identify the position of the optimal operational point; and providing recommendations based on the attained results regarding the compression of medical images corrupted by Poisson noise using a BPG encoder, with the aim of maximizing the restored image's quality resemblance to the original. The employed **methods** encompass image quality assessment techniques employing MSE, PSNR, MSSIM, and PSNR-HVS-M metrics, as well as software modeling in Python without using the built-in Poisson noise generator. The ensuing **results** indicate that optimal operational points (OOP) can be discerned for all these metrics when the compressed image quality surpasses that of the corresponding original image, accompanied by a sufficiently high compression ratio. Moreover, striking a suitable balance between the compression ratio and image quality leads to partial noise reduction without introducing notable distortions in the compressed image. This study underscores the significance of employing appropriate metrics for evaluating the quality of compressed medical images and provides insights into determining the compression parameter Q to attain the BPG encoder's optimal operational point for specific images. **Conclusions.** The scientific novelty of the findings encompasses the following: 1) the capability of all metrics to determine the OOP for images of moderate visual complexity or those dominated by homogeneous areas; MSE and PSNR metrics demonstrating superior results for images rich in textures and edges; 2) the research highlights the dependency of Q in the OOP on the average image intensity, which can be reasonably established for a given image earmarked for compression based on our outcomes. The compression ratios for images compressed at the OOP are sufficiently high, further substantiating the rationale for compressing images in close proximity to the OOP.*

Keywords: lossy image compression; BPG; Poisson noise; optimal operation point.

Introduction

Medical image compression is highly relevant in the field of healthcare because it can significantly improve the efficiency and cost-effectiveness of medical imaging. With the increasing use of digital imaging technologies in medical diagnosis and treatment, the size of medical image datasets has also increased, leading to challenges in storing, transmitting, and processing these images [1]. Medical image compression techniques can help address these challenges by reducing the storage and transmission requirements of medical images without compromising their diagnostic quality [2, 3]. This can lead to faster and more reliable diagnoses, reduced storage and transmission costs, and improved patient care. In addition, medical image compression is crucial for telemedicine and remote medical services, where efficient transmission of medical images is critical for timely diagnosis and treatment.

There are two types of compression commonly used in digital image processing: lossless and lossy compression [4]. Lossless compression, as the name suggests, allows a compressed image file to be restored to its original state without any loss of data. This technique is commonly used in medical imaging applications where even the slightest loss of image data could have significant consequences on diagnosis and treatment decisions [5, 6]. Lossy compression [7-10], on the other hand, involves the removal of certain image data to achieve higher compression rates. Although this technique results in smaller file sizes, it also leads to some loss of image quality, which may not be acceptable in medical imaging applications [11-14].

Regarding medical image compression, there are special requirements that must be considered. First, the compressed images must be able to preserve the diagnostic quality of the corresponding original images. In addition, medical images must be compressed in a manner

that allows for fast and efficient transmission and storage, while also meeting the security and privacy requirements of the healthcare industry. Finally, the compressed images must be compatible with various medical imaging software and hardware systems to ensure seamless integration into clinical workflows. Meeting these requirements is crucial to ensure that compressed medical images can be used effectively in clinical settings [15, 16].

However, these are not the only problems that can be faced. In addition, the noise in acquired images can significantly affect image quality. Such noise masks the details of the images.

Medical imaging systems, such as X-ray and computed tomography (CT) use X-rays or CT scans to generate images of the patient's region of interest, which are recorded by measuring the resulting attenuation [17]. The noise probability density function in images acquired by these systems is often modeled by the Poisson distribution and is commonly known as Poisson noise, shot noise, photon noise, Schott noise, or quantum noise. Poisson noise is unique in that it is not influenced by temperature or frequency but rather by photon counting. The strength of Poisson noise is directly proportional to the pixel intensity: higher-intensity pixels exhibit greater noise variance than lower-intensity pixels [18].

Special approaches are required when compressing images in the presence of noise. Lossless compression is particularly affected by noise, which can greatly reduce the achieved compression ratio (CR) [19]. Therefore, it is recommended to use lossy compression, which offers higher CR values and several other advantages.

One of these advantages is the noise-filtering effect achieved by setting certain parameters specifically. This effect was first observed in [20-22], and it occurs for compression methods that use various orthogonal transforms [17-20]. One important task is to choose encoder parameters such that compression is performed near the optimal operating point (OOP) [20, 23-26], which ensures that the decoded image is as close as possible to the original image based on the chosen criterion. The existence of the optimal operating point (OOP) has been demonstrated for various types of noise [20], compression methods based on discrete cosine transform (DCT) [27, 28], and wavelets [22]. Different criteria such as mean-square error (MSE) and peak signal-to-noise ratio (PSNR) [21, 24], as well as metrics that consider visual quality such as PSNR-HVS-M and MSSIM [29], can be used to determine the OOP. However, the automatic provision of compression near the OOP for complex types of signal-dependent interference remains a challenge.

The issue of automatic provision of compression in the vicinity of the OOP has been successfully addressed for additive and mixed noise, as shown in [25, 30]. However, the situation is more challenging for simple types of signal-dependent noise, such as multiplicative and Poisson noise. It is worth noting that the practical relevance of studying the impact of complex signal-dependent noise characteristics on lossy image compression has increased in recent times. Such models have been acknowledged as more suitable, particularly for medical images produced by devices such as X-rays and computed tomography. Therefore, the objectives of this article are to investigate the properties of BPG lossy compression for images corrupted by Poisson noise depending on image content and characteristics and to provide guidelines (recommendations) for selecting the compression parameters.

The paper structure is as follows. First, we consider image/noise models. Then, the criteria of compression efficiency are discussed with special attention to visual quality. The advantages of the BPG coder are briefly refreshed. Simulation results in a set of test images are presented and discussed. Several illustrations demonstrating the specific features of lossy compression of noisy images are presented. Finally, the conclusions follow.

1. Image and noise models

When evaluating image compression techniques for noisy images, it is crucial to consider both the image model and the noise model. Understanding the impact of noise on the compression process requires defining the statistics of the noise. Signal-dependent noise, for instance, can have a very different effect on compression than signal-independent noise. To properly address the influence of noise, the noise model should accurately describe the noise properties. In addition, restoring images that have been degraded by noise depends on both the image and noise models. The validity and effectiveness of restoration techniques are highly influenced by the models used.

1.1. Noise model

This study used the Gaussian Approximation of the Poisson Distribution from [31].

For large mean values, the Poisson distribution is well approximated by a Gaussian distribution with the mean and variance equal to the mean of the Poisson random variable:

$$P(\mu) \approx N(\mu, \mu),$$

where N – is the normal distribution with expected value μ.

In the study [31], the authors present an intuitive proof that leverages the Central Limit Theorem (CLT)

and the closure property of Poisson distributions with respect to the summation of variables. When modeling Poisson noise, you can use both special options available in many tools and model it as Gaussian noise with a variance equal to the true value in a pixel, which is true for image true values of at least 12.

Using the aforementioned approximation, it becomes feasible to substitute the Poisson distribution family with a Gaussian distribution family that has a non-constant (spatially varying) variance that is dependent on the true value of the signal (image pixel). This approximation is attractive in modeling because it can often simplify the analysis and processing procedures, including noise estimation and denoising. We simulated Poisson noise by scaling a normally distributed noise signal with zero mean and unity variance by the square root of the expected signal value (μ), and then adding it to the image.

1.2. Image model

Medical imaging involves various techniques to create visual representations of the human body through the processing of biomedical signals. The resulting still images differ depending on the imaging method and the anatomical part being examined, resulting in a range of image features.

The performance of image compression techniques heavily relies on the characteristics of the image being compressed, whether it contains noise or not. Hence, selecting appropriate test images is crucial, considering varying complexity and noise-free qualities. Visually simple structure images are generally compressed with less loss, producing higher quality at a given compression ratio for a selected method and better noise reduction. In contrast, complex structure images exhibit opposite properties. Our research involved testing six images, including ankle.png, head_tumour.png, leg_veins.png, pelvis.png, spine.png, and wrist.png. The test images used were obtained from the website https://radiopaedia.org/, and they represent medical images of atypical diagnostic cases.

To simulate a real-world scenario, these images were artificially distorted with noise generated according to the previously mentioned model. Figure 1 displays the original wrist.png image (a) and the corresponding noisy version (b). and Figure 2 displays the original head_tumour.png image (a) and the corresponding noisy version (b). Noise is clearly visible in image regions with high mean intensity (light gray ones) and practically invisible in dark regions.

2. Lossy Compression Efficiency

One characteristic of lossy compression applied to noisy images is its capability to suppress noise when specific control parameters are configured, allowing the compression of images near the OOP. To evaluate the effectiveness of compression and noise suppression, traditional quality criteria such as MSE are employed alongside metrics related to visual quality, including PSNR-HVS-M and MSSIM. These criteria necessitate a comparison between the decompressed noisy image Idec and the original, noise-free image Iorig for a group of test images that were distorted by artificially generated noise.

The primary objective of lossy image compression is to achieve an acceptable level of quality while maximizing CR.

Therefore, we must strike a balance between the compression ratio and image quality, as increasing the CR will inevitably introduce larger distortions into the compressed image. If lossy compression is applied to a noisy image, the introduced distortions can relate to both suppressed noise and edge/detail/texture smearing. Thus, a specific analysis must be performed.


a

b

Fig. 1. Example of the original (a)
and noisy (b) images

## 2.1. Used quality metrics

A conventional approach to rate-distortion curve (RDC) obtaining and analysis is to compress an image with a set of values of a parameter that controls compression (PCC) and to estimate a metric used in the analysis for the considered set of PCC values.

For the BPG encoder, the parameter Q is employed as PCC where PCC increase leads to a larger CR and larger distortions. In this sense, RDCs obtained for (noisy) images subject to compression and the corresponding compressed images depending on Q behave in a traditional manner – metric values become worse (MSE reduces, PSNR, MS-SSIM, and PSNR-HVS-M increase) if Q increases.
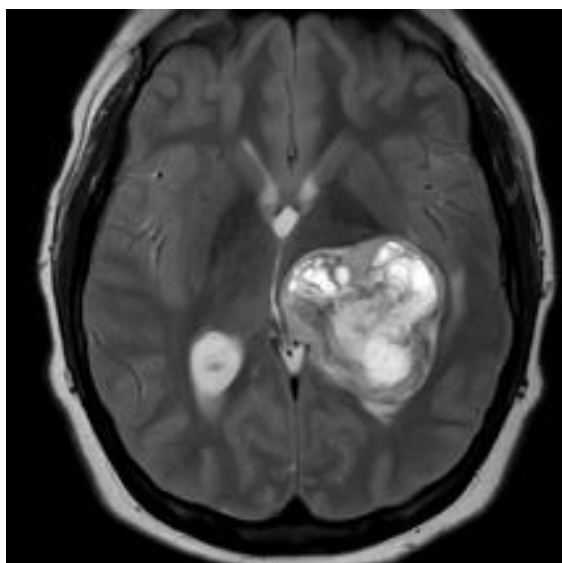
a
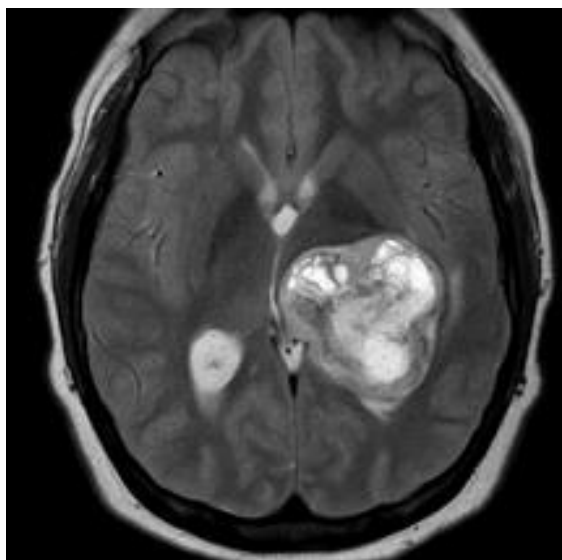
b

Fig. 2. Example of the original (a)
and noisy (b) images

Meanwhile, we are more interested in other types of dependencies that can be obtained only in simulations. In fact, to determine the optimal CR, we have to establish an RDC by comparing the true image (without noise) I_{ij}^{tr}, $i = 1,...,I$, $j = 1,...,J$ to the compressed (originally noisy) image at different compression parameter values using a criterion or metric. Having a compressed image I_{ij}^{c}, $i=1,...,I$, $j =1,...,J$ it is easy to calculate

$$MSE_{tc} = \frac{1}{IJ}\sum_{i=1}^{I}\sum_{j=1}^{J}(I_{ij}^{tr} - I_{ij}^{c})^2, \qquad (1)$$

where I_{ij}^{tr}, I_{ij}^{c} – pixel brightness value of true and compressed images, respectively; $I \times J$ – image size.

$$PSNR_{tc} = 10\log_{10}\left(\frac{255^2}{MSE_{tc}}\right). \qquad (2)$$

The coordinates of the global minimum of the MSE_{tc} metric and the maximum of the $PSNR_{tc}$ metric are OOP in the conventional sense. Compression in OOP is also worth characterizing by the compression ratio because this parameter is also important in practice.

The PSNR-HVS-M metric takes into account the features of the human visual system and is based on the discrete cosine transform (DCT). PSNR-HVS-M metric values are measured in decibels, larger values correspond to better visual quality.

The MSSIM metric is based on the wavelet transform and ranges from 0 (very poor quality) to 1 (excellent quality).

Since the visual quality of compressed images is extremely important for the considered application, it is worth analyzing the dependencies of visual quality metrics on Q as well.

2.2. The considered compression method

The founder of QEMU and FFmpeg, Fabrice Bellard, created a new lossy image format called BPG. It uses the HEVC compression algorithm, offers a higher compression ratio with a similar quality to JPEG, supports different color formats, and offers both lossless and lossy compression. BPG encoder performs DCT in 64 × 64 blocks with minimum recursive block partitions of 4 × 4 pixels, uses DCT transformation to the frequency domain, and entropy coding to eliminate redundancy. A source code package with a command line encoder, decoder, and library is also provided.

To determine the optimal quantization step (Q), which serves as PCC for the BPG encoder, at which the noise suppression effect manifests itself in the best manner and OOP is observed, we consider the compression of the test images in the Q range from 1 to 50 with a step of 1 (Fig. 3).

3. Results and Discussion

3.1. Results for conventional metrics

We start our analysis from the conventional MSE metric (1). Fig. 3, a shows data obtained for original test images. Since it difference in behavior depending on $MSE_{tc}(Q_S=1)$ has been immediately noticed, we have also created an additional set of test images for which $I_{ij}^{trnew} = I_{ij}^{tr}/2$, i $=1,...,I$ j $=1,...,J$, i.e. new images are "darker". The obtained results are presented in Fig. 3, b.

As can be seen from the dependencies shown in Fig. 3, the MSE_{tc} varies over a wide range. For a small Q (<23), MSE_{tc} for a given image remains practically the same. A further increase in Q leads to smaller values in the vicinity of the OOP for all six images in Fig. 3, a and all six images in Fig. 3, b. Here partial noise suppression is observed, which is characterized by a decrease in the MSE_{tc}. Then, for a larger Q, MSE_{tc} steadily increases if Q becomes larger.
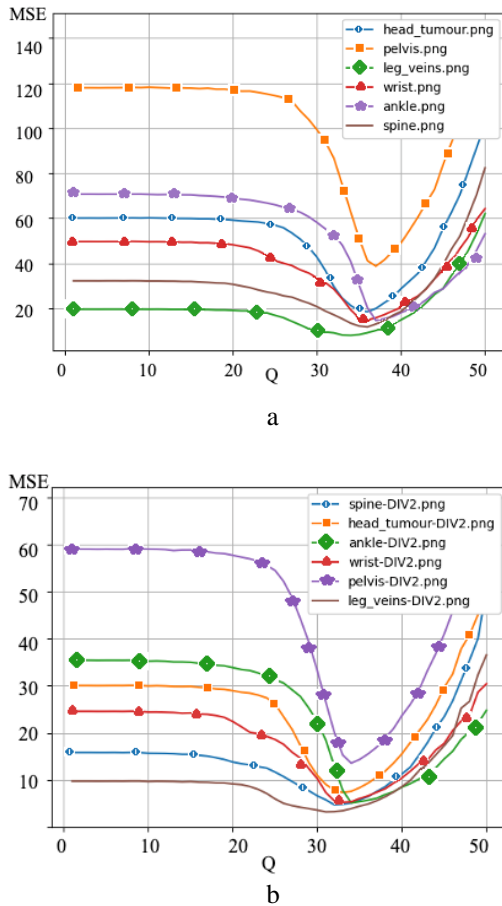

a

b

Fig. 3. Dependencies of MSE_{tc} on Q
for the test images compressed by BPG encoder

Another observation is that for images with a smaller number of texture areas (leg_veins.png, spine.png), the MSE_{tc} values are significantly lower than

those for high-texture images (pelvis.png). Accordingly, the filtering effect is greater for them.

An interesting observation is that Q for optimal operation point (Q_{OOP}) is related to $MSE_{tc}(QS=1)$: for a larger $MSE_{tc}(Q=1)$, Q_{OOP} is also larger. Note that $MSE_{tc}(Q=1)$ corresponds to the case in which practically no compression is applied.

Thus, $MSE_{tc}(Q=1)$ approximately corresponds to the "equivalent" noise variance of Poisson noise. It is easy to show that this equivalent variance is approximately equal to the image mean where the image mean values can be determined for both the true and noisy images (they are practically the same). Thus, Q_{OOP} depends on the image mean, at least, for the metrics MSE_{tc} and, respectively, $PSNR_{tc}$ (see Fig. 4).

According to the $PSNR_{tc}$ metric (Fig. 4), the coordinates of the maxima coincide with the corresponding coordinates of the minima of the MSE_{tc} metric. OOP is less prominent in images with more texture objects and edges (pelvis.png). Simple images such as leg_viens.png and spine.png have a more pronounced OOP. Q_{OOP} is larger for images having a smaller $PSNR_{tc}(Q=1)$. This occurs for all images, the plots for which are presented in Figures 4, a and 4, b. Note that, for some images compressed in OOP, the distortions and residual noise are practically invisible – this happens if PSNR exceeds 36 dB.
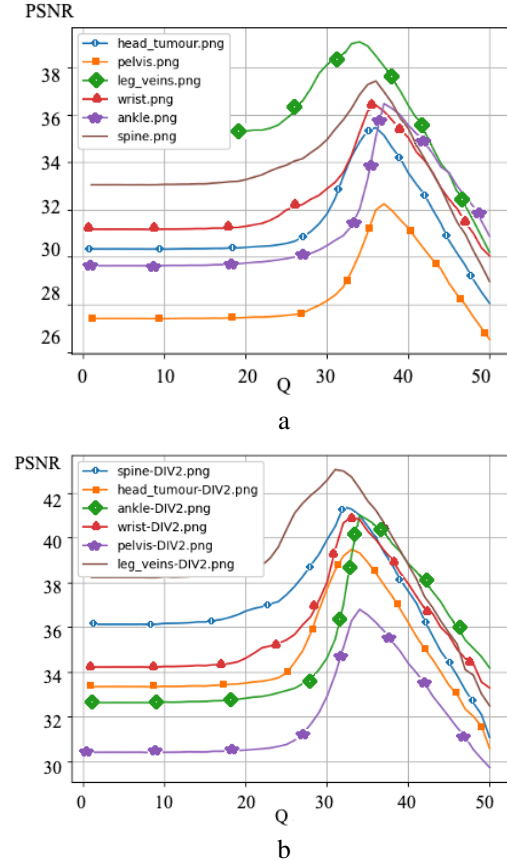

a

b

Fig. 4. Dependences of $PSNR_{tc}$ metric values on Q
for the test images compressed by the BPG

3.2. Results for the visual quality metrics

According to the MS-SSIM$_{tc}$ metric (Fig. 5), OOPs are also observed, and this occurs for all six test images in both Figures. It is also worth noting that the coordinates of the maxima almost coincide with the corresponding coordinates of the minima of the MSE$_{tc}$ metric.

It might seem that OOP is more pronounced for images with many texture objects and borders (pelvis.png, head_tumour.png, ankle.png). For simple images, OOP is less pronounced (leg_veins.png, spine.png). However, it is necessary to keep in mind that MS-SSIM is a very nonlinear metric.
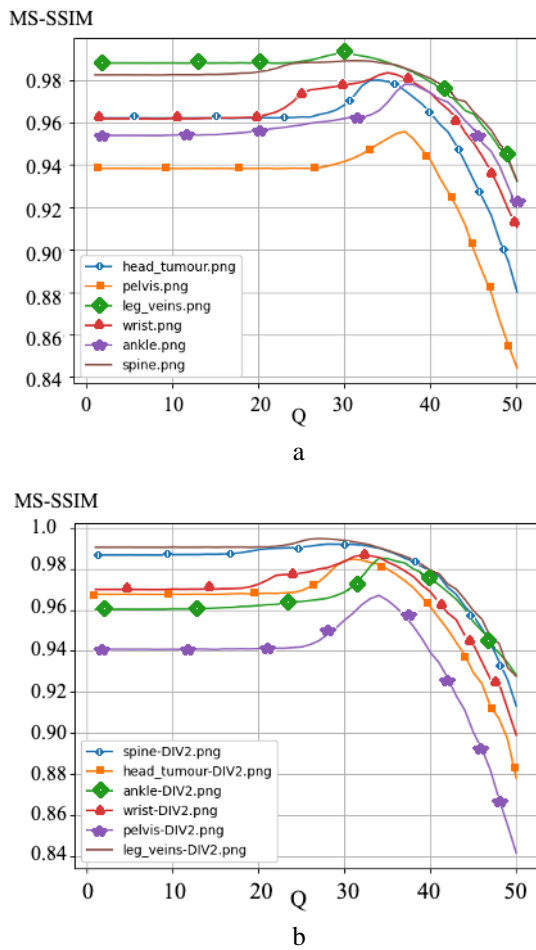

a

b

Fig. 5. Dependences of MS-SSIM$_{tc}$ on Q
for the test images compressed by the BPG encoder

Finally, let us analyze the data for the metric PSNR-HVS-M or, equivalently, MSE-HVS-M (PSNR-HVS-M=$10\log_{10}$ (255^2 / MSE-HVS-M); see the plots in Fig. 6). Analysis shows that the minima coordinate (Q$_{OOP}$) nearly matches the minima coordinates of the MSE$_{nc}$ metric. The OOP is not very clear for images with more texture objects and edges (pelvis.png). For images such as leg_viens.png and spine.png, the OOPs are not

observed. Thus, OOPs occur more rarely for visual quality metrics than for conventional metrics such as MSE or PSNR.

For practice, we are interested in two more things. First, can we predict (without having I$_{ij}^{tr}$, i =1,...,I, j =1,...,J at disposal as this happens in practice) what is Q$_{OOP}$ for a given image corrupted by Poisson noise? Second, what are CR values that can be reached if a noisy image is compressed in OOP?

To answer both questions, we conducted a special study. Table 1 shows the Q values corresponding to the OOP according to the MSE and MS-SSIM metrics. It is easy to see that the discrepancy between the OOP values determined by different metrics ranges from 0 to 4. It is also seen that for images with the -DIV2 suffix, which are the transformations of the image of the same name by dividing each pixel value by 2, the position of the OOP is shifted by 2 or 3 to the smaller side. The general tendency is that Q$_{OOP}$ is larger for images with a larger mean. The presented data already allow for initial recommendations on the determination of Q$_{OOP}$, but, in our opinion, more test images are needed to obtain a proper regression.
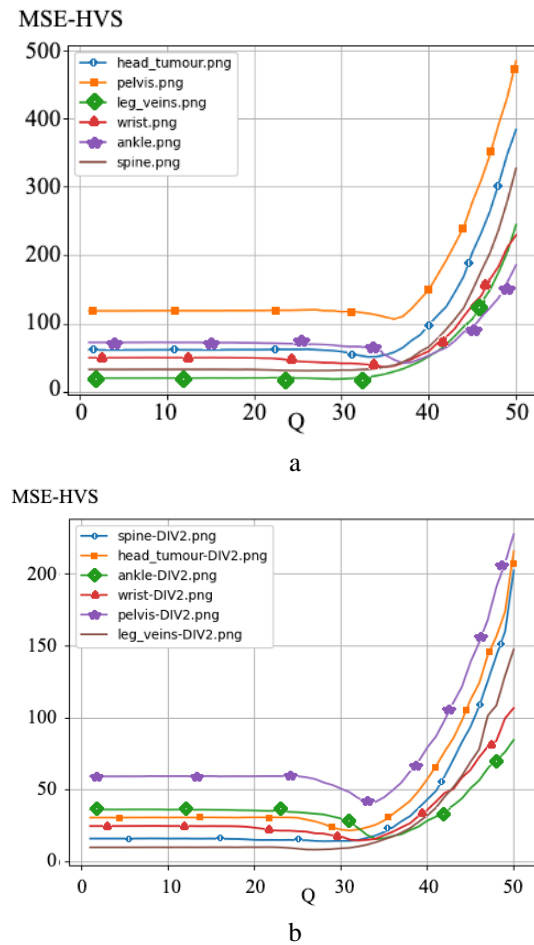

a

b

Fig. 6. Dependencies of MSE-HVS-M$_{tc}$ on Q
for the test images compressed by the BPG encoder

Table 1 also displays the compression ratio for the corresponding OOPs for each test image. The results indicate that relying on the OOP determined by the MS-SSIM metric results in a compression ratio that is either equal to the CR determined by the MSE metric or less than 10-22. Thus, it can be concluded that determining of the OOP according to the MSE metric or setting the Q parameter as Q_{OOP} (MS-SSIM) + 3 is reasonable for achieving a higher compression ratio.

Examples of compression for two test images at the optimal operating point and at a random point with a smaller Q are shown in Fig. 7 and 8.

Table 1

The position of the optimal operating point according to the MSE and MS-SSIM metrics

| Image name	Image mean	Q_{OOP} (MSE_{tc})	CR_{OOP} (MSE_{tc})	Q_{OOP} (MS-SSIM)	CR_{OOP} (MS-SSIM)
head_tumour.png	60.5	36	37.95	34	23.11
head_tumour-DIV2.png	30.05	33	29.29	31	16.4
pelvis.png	118.53	37	41.36	37	41.36
pelvis-DIV2.png	59.01	34	32.64	34	32.64
leg_veins.png	19.83	34	35.56	30	14.66
leg_veins-DIV2.png	9.80	31	27.81	27	10.47
ankle.png	71.54	37	63.20	37	63.20
ankle-DIV2.png	35.53	34	48.61	34	48.61
wrist.png	49.76	36	52.67	35	38.83
wrist-DIV2.png	24.63	33	39.35	32	28.21
spine.png	32.50	36	44.01	32	18.83
spine-DIV2.png	16.00	32	31.54	30	17.58

a
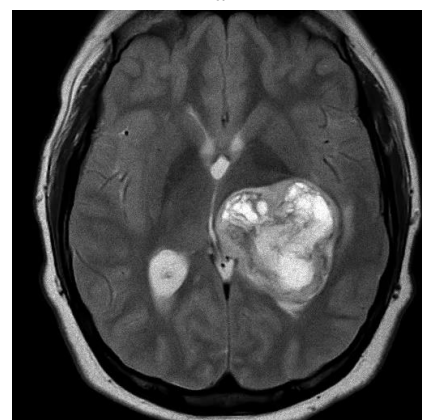

b

Fig. 7. An example of decompressed test images compressed near the OOP (Q = 35) (a), (c) and at a random point (Q = 27) (b), (d)
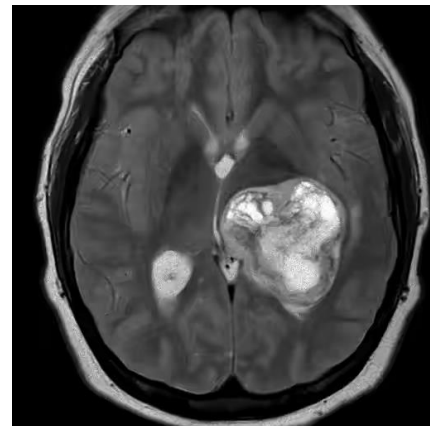
a

b

Fig. 8. An example of decompressed test images compressed near the OOP (Q = 35) (a), (c) and at a random point (Q = 27) (b), (d)

3.3. Brief discussion

It can be observed (Fig. 8, b) that when compressing images with Q_{OOP}, the decompressed images are almost noise-free (denoised well), whereas compressing with a smaller Q does not produce this effect. This means that denoising might be applied after compression with $Q<Q_{OOP}$.

Analysis of the data in Table 1 also shows that dependence of Q_{OOP} on image mean might exist since a general tendency seems to be Q_{OOP} increasing if the image mean becomes larger. In addition, if the visual quality of compressed images is of prime importance, Q can be set slightly smaller than Q_{OOP} according to conventional metrics.

CR values for image compression in OOP and its neighborhood are quite large. At least, they are by the order of magnitude larger than if noisy images are subject to lossless compression (then, CR is usually less than 1.5). Thus, compression in OOP has obvious advantages. Meanwhile, as it follows from the analysis of dependencies in Fig. 6, there exist images for which OOP is absent or "is not obvious" (see the curves for the image leg_veins).

Conclusions

We analyzed the peculiarities of lossy compression of noisy medical images using a BPG encoder. It is shown that OOP almost always exists according to MSE and PSNR metrics and is often observed for the considered visual quality metrics. It is demonstrated that Q_{OOP} depends on image mean intensity, and it is quite easy to determine Q_{OOP} for a given image to be compressed using the data in Table 1.

The main contribution of this paper is that we have demonstrated the existence of OOP for most images contaminated by Poisson noise and compressed by the BPG coder. This happens due to the noise filtering effect that occurs due to lossy compression. The results presented in Table 1 allow Q to be chosen depending on the image mean.

Note that CR values for images compressed in OOP are quite large, which makes it reasonable to compress images in the vicinity of OOP.

In the future, we plan to consider opportunities for post-filtering compressed images and applying lossy compression to already pre-filtered images.

Contributions of authors: conceptualization, methodology – **Volodymyr Lukin**; formulation of tasks, analysis – **Volodymyr Lukin**; development of model, software, verification – **Victoriia Naumenko**; analysis of results, visualization – **Bogdan Kovalenko**; writing – original draft preparation, writing – review and editing – **Victoriia Naumenko**.

All the authors have read and agreed to the published version of this manuscript.

References

1. Ng, K. H., Faust, O., Sudarshan, V., & Chattopadhyay, S. Data Overloading in Medical Imaging: Emerging Issues, Challenges and Opportunities in Efficient Data Management. *Journal of Medical Imaging and Health Informatics*, 2015, vol. 5, iss. 4, pp. 755–764. DOI: 10.1166/jmihi.2015.1449.

2. Patidar, G., Kumar, S., & Kumar, D. A Review on Medical Image Data Compression Techniques. *2nd International Conference on Data, Engineering and Applications (IDEA),* Bhopal, India, 2020, pp. 1-6. DOI: 10.1109/IDEA49133.2020.9170679.

3. Kumar, S., & Kumar, D. Comparative Analysis and Performance Evaluation of Medical Image Compression Method for Telemedicine. *2nd International Conference on Data, Engineering and Applications (IDEA),* Bhopal, India, 2020, pp. 1-5. DOI: 10.1109/IDEA49133.2020.9170724.

4. Hussain, A. J., Al-Fayadh, A., & Radi, N. Image Compression Techniques: A Survey in Lossless and Lossy algorithms. *Neurocomputing,* 2018, vol. 300, pp. 44-49. DOI: 10.1016/j.neucom.2018.02.094.

5. Kryvenko, S., Lukin, V., Krylova, O., Kryvenko, L., & Egiazarian, K. A Fast Method of Visually Lossless Compression of Dental Images. *Applied Sciences,* 2021, vol. 11, iss. 1, article no. 135. DOI: 10.3390/app11010135.

6. Kumar, S. N., Haridhas, A. K., Fred, A. L., & Varghese, P. S. Analysis of Lossy and Lossless Compression Algorithms for Computed Tomography Medical Images Based on Bat and Simulated Annealing Optimization Techniques. *Computational Intelligence Methods for Super-Resolution in Image Processing Applications.* Springer, Cham., 2021, pp. 99-133. DOI: 10.1007/978-3-030-67921-7_6.

7. Moura, L., Furuie, S. S., Gutierrez, M. A., Tachinardi, U., Rebelo, M. S., Alcocer, P., & Melo, C. P. Lossy compression techniques, medical images, and the clinician. *MD Computing : computers in medical practice,* 1996, vol. 13, iss. 2, pp. 155-172. PMID: 8684278.

8. Sultana, Z., Nahar, L., Tasnim, F., Hossain, M. S., & Andersson, K. Lossy Compression Effect on Color and Texture Based Image Retrieval Performance. *Intelligent Computing & Optimization. ICO 2022. Lecture Notes in Networks and Systems,* Springer, Cham., 2023, vol. 569, pp. 1159-1167. DOI: 10.1007/978-3-031-19958-5_108.

9. European Society of Radiology (ESR). Usability of irreversible image compression in radiological imaging. A position paper by the European Society of Radiology (ESR). *Insights into Imaging,* 2011, vol. 2, iss. 2, pp. 103-115. DOI: 10.1007/s13244-011-0071-x.

10. Barannik, V., Sidchenko, S., Barannik, D., Yermachenkov, A., Savchuk, M., & Pris, G. Video images compression method based on floating positional coding with an unequal codograms length. *Radioelectronic and Computer Systems*, 2023, no. 1, pp. 134-146. DOI: 10.32620/reks.2023.1.11.

11. Liu, F., Hernandez-Cabronero, M., Sanchez, V., Marcellin, M. W., & Bilgin, A. The Current Role of Image Compression Standards in Medical Imaging. *Information,* 2017, vol. 8, iss. 4, article no. 131. DOI: 10.3390/info8040131.

12. *Guidance for the content and review of 510(K) Notifications for Picture Archiving and Communications Systems (PACS) and Related Devices*. Food and Drug Administration. 2023. Available at: https://www.accessdata.fda.gov/scripts/cdrh/cfdocs/cfpmn/pmn.cfm?ID=K211257. (accessed 12.06.2023).

13. Lukin, V., Bataeva, E., & Abramov, S. Saliency map in image visual quality assessment and processing. *Radioelectronic and computer systems,* 2023, no. 1, pp. 112-121. DOI: 10.32620/reks.2023.1.09.

14. Bondžulić, B., Pavlović, B., Stojanović, N., & Petrović, V. Picture-wise just noticeable difference prediction model for JPEG image quality assessment. *Vojnotehnicki glasnik,* 2022, vol. 70, iss. 1, pp. 62-86. DOI: 10.5937/vojtehg70-34739.

15. Gooden, D. S. Legal aspects of image compression. *In Proceedings of the American Assoc. of Physicists in Medicine (AAPM). 35th Annual Meeting,* Washington, DC, 1993, pp. 8-12.

16. Koff, D., Bak, P., Brownrigg, P. et al. Pan-Canadian evaluation of irreversible compression ratios ("lossy" compression) for development of national guidelines. *Journal of digital imaging,* 2009, vol. 22, pp. 569-578. DOI: 10.1007/s10278-008-9139-7.

17. Prasath, V. B. S. Quantum Noise Removal in XRay Images with Adaptive Total Variation Regularization, *Informatica,* 2017, vol. 28, iss. 3, pp. 505-515. DOI: 10.15388/Informatica.2017.141.

18. Le, T., Chartrand, R., & Asaki, T. J. A Variational Approach to Reconstructing Images Corrupted by Poisson Noise. *Journal of Mathematical Imaging and Vision*, 2007, vol. 3, pp. 257-263. DOI: 10.1007/s10851-007-0652-y.

19. Li, B., Yang, R., & Jiang, H. Remote-Sensing Image Compression Using Two-Dimensional Oriented Wavelet Transform. *IEEE Transactions on Geoscience and Remote Sensing,* 2011, vol. 49, iss. 1, pp. 236-250. DOI: 10.1109/TGRS.2010.2056691.

20. Al-Chaykh, O. K., & Mersereau, R. M. Lossy compression of noisy images. *IEEE Transactions on Image Processing,* 1998, vol. 7, iss. 12, pp. 1641-1652. DOI: 10.1109/83.730376.

21. Shahnaz, R., Walkup, J. F., & Krile T. F. Image Compression in Signal-Dependent Noise. *Applied Optics,* 1999, vol. 38, iss. 26, pp. 5560-5567. DOI: 10.1364/AO.38.005560.

22. Chang, S. G., Yu, B., & Vetterli, M. Adaptive wavelet thresholding for image denoising and compression. *IEEE Trans. on Image Processing,* 2000, vol. 9, iss. 9, pp. 1532-1546. DOI: 10.1109/83.862633.

23. Lim, S. H. Characterization of Noise in Digital Photographs for Image Processing. *Proceedings of Digital Photography II,* 2006, vol. 60690O, pp. 219-228. DOI: 10.1117/12.655915.

24. Lukin, V., Kovalenko, B., Kryvenko, S., Naumenko, V., & Vozel, B. Prediction of Optimal Operation Point Existence and Its Parameters in BPG-Based Automatic Lossy Compression of Noisy Images. *Current Overview on Science and Technology Research,* 2022, vol. 9, pp. 1-36. DOI: 10.9734/bpi/costr/v9/4316A.

25. Kovalenko, B., Lukin, V., Kryvenko, S., Naumenko, V., & Vozel, B. BPG-Based Automatic Lossy Compression of Noisy Images with the Prediction of an Optimal Operation Existence and Its Parameters. *Applied Sciences,* 2022, vol. 12, iss. 15, article no. 7555. DOI: 10.3390/app12157555.

26. Naumenko, V., Lukin, V., & Krivenko, S. Analysis of Noisy Image Lossy Compression by BPG. *Integrated Computer Technologies in Mechanical Engineering – 2021. ICTM 2021. Lecture Notes in Networks and Systems,* Springer, Cham, 2022, vol. 367, pp. 911-923. DOI: 10.1007/978-3-030-94259-5_71.

27. Makarichev, V., Lukin, V., & Brysina, I. Progressive DCT-based coder and its comparison to atomic function based image lossy compression. *IEEE 16th International Conference on Advanced Trends in Radioelectronics, Telecommunications and Computer Engineering (TCSET)*, Lviv-Slavske, Ukraine, 2022, pp. 01-06, DOI: 10.1109/TCSET55632.2022.9766871.

28. Li, F., Krivenko, S., & Lukin, V. A Two-step Procedure for Image Lossy Compression by ADCTC with a Desired Quality. *IEEE 11th International Conference on Dependable Systems, Services and Technologies (DESSERT)*, Kyiv, Ukraine, 2020, pp. 307-312. DOI: 10.1109/DESSERT50317.2020.9125000.

29. Wang, Z., Simoncelli, E. P., & Bovik, A. C. Multiscale structural similarity for image quality assessment. *The Thrity-Seventh Asilomar Conference on Signals, Systems & Computers,* 2003, vol. 2, Pacific Grove, CA, USA, 2003, pp. 1398-1402. DOI: 10.1109/ACSSC.2003.1292216.

30. Lukin, V. V., Krivenko, S. S., Zriakhov, M. S., Ponomarenko, N. N., Abramov, S. K., Kaarna, A., & Egiazarian, K. Lossy compression of images corrupted by mixed Poisson and additive Gaussian noise. *2009 International Workshop on Local and Non-Local Approximation in Image Processing*, Tuusula, Finland, 2009, pp. 33-40. DOI: 10.1109/LNLA.2009.5278407.

31. Azzari, L., Borges, L. R., & Foi, A. Modeling and Estimation of Signal-Dependent and Correlated Noise. *Denoising of Photographic Images and Video. Advances in Computer Vision and Pattern Recognition*. Springer, Cham, 2018, pp. 1-36. DOI: 10.1007/978-3-319-96029-6_1.

АНАЛІЗ СТИСНЕННЯ НА ОСНОВІ BPG МЕДИЧНИХ ЗОБРАЖЕНЬ
З ШУМОМ ПУАССОНА

Вікторія Науменко, Богдан Коваленко,
Володимир Лукін

Предмет дослідження – стиснення з втратами з використанням кодера BPG для медичних зображень з різними рівнями візуальної складності, зіпсованих шумом Пуассона. **Мета** полягає у визначенні оптимальних параметрів для стиснення зображень та підборі найбільш підходящої метрики для визначення оптимальної робочої точки. Вирішувані **завдання** включають: вибір тестових зображень розміром 512x512 в градаціях сірого з різними рівнями візуальної складності, що включають у себе візуально складні зображення з багатьма кордонами та текстурами, помірно складні зображення з кордонами та текстурами поруч з однорідними областями та візуально прості зображення, що складаються переважно з однорідних областей; вибір метрик оцінки якості зображень та оцінка їх поведінки для різних параметрів стиснення кодера; вибір однієї чи декількох метрик, які чітко визначають позицію оптимальної робочої точки; надання рекомендацій на основі отриманих результатів щодо стиснення медичних зображень, зіпсованих шумом Пуассона, використовуючи кодер BPG, з метою максимізації якості відновленого зображення в порівнянні з оригіналом. Використані **методи** включають техніки оцінки якості зображень за допомогою метрик MSE, PSNR, MSSIM та PSNR-HVS-M, а також програмне моделювання на мові Python без використання вбудованого генератора шуму Пуассона. Отримані **результати** свідчать про те, що оптимальні робочі точки (ОРТ) можуть бути визначені для всіх цих метрик, коли якість стисненого зображення перевершує якість відповідного оригіналу, що також супроводжується достатньо високим ступенем стиснення. Крім того, досягнення відповідності між ступенем стиснення та якістю зображення сприяє частковому зменшенню шуму без значних спотворень на стисненому зображенні. Дослідження підкреслює важливість використання відповідних метрик для оцінки якості стиснених медичних зображень та надає висновки щодо визначення параметра компресії Q для досягнення оптимальної операційної точки кодера BPG для конкретних зображень. **Висновки.** Наукова новизна отриманих результатів полягає в наступному: 1) здатність всіх метрик визначити ОРТ для зображень помірної візуальної складності або тих, що мають переважно однорідні області; метрики MSE та PSNR демонструють кращі результати для зображень з багатими текстурами та кордонами; 2) дослідження підкреслює залежність Q від ОРТ від середньої інтенсивності зображення, яка може бути розумно встановлена для даного зображення, що стискається, на основі наших результатів. Значення коефіцієнта стиснення для зображень, стиснутих в ОРТ, досить великі, що є додатковим аргументом для стиснення зображень поблизу ОРТ.

Ключові слова: стиснення зображення з втратами; BPG; шум Пуассона; оптимальна робоча точка.

Науменко Вікторія Володимирівна – канд. техн. наук, доц. каф. інформаційно-комунікаційних технологій ім. О. О. Зеленського, Національний аерокосмічний університет ім. М. Є. Жуковського «Харківський авіаційний інститут», Харків, Україна.

Коваленко Богдан Віталійович – асп. каф. інформаційно-комунікаційних технологій ім. О. О. Зеленського, Національний аерокосмічний університет ім. М. Є. Жуковського «Харківський авіаційний інститут», Харків, Україна.

Лукін Володимир Васильович – д-р техн. наук, проф., зав. каф. інформаційно-комунікаційних технологій ім. О. О. Зеленського, Національний аерокосмічний університет ім. М. Є. Жуковського «Харківський авіаційний інститут», Харків, Україна.

Victoriia Naumenko – PhD of Technical Science, Associate Professor of the Department of Information- communication technologies named after O. O. Zelensky, National Aerospace University "Kharkiv Aviation Institute", Kharkiv, Ukraine,
e-mail: v.naumenko@khai.edu, ORCID: 0000-0002-5291-6032, Scopus Author ID: 55847192600.

Bogdan Kovalenko – PhD Student of the Department of Information-communication Technologies named after O. O. Zelensky, National Aerospace University "Kharkiv Aviation Institute", Kharkiv, Ukraine,
e-mail: b.kovalenko@khai.edu, ORCID: 0000-0002-9360-0691.

Volodymyr Lukin – Doctor of Technical Science, Professor, Head of the Department of Information-communication technologies named after O. O. Zelensky, National Aerospace University "Kharkiv Aviation Institute", Kharkiv, Ukraine,
e-mail: v.lukin@khai.edu, ORCID: 0000-0002-1443-9685.